Journal of ELECTRICAL ENGINEERING, VOL 73(2022), NO6, 413–418

sciendo

PAPERS

Characteristic-mode analysis of coupled split-ring resonators

Akaa Agbaeze Eteng[1]

The coupling between closely spaced split-ring resonators, when employed as sub-components of electromagnetic structures, is an important feature often leveraged upon to provide bulk material properties. In its contribution, this paper employs characteristic-mode analysis (CMA) to examine modal interactions intrinsic to the coupling between a pair of split-ring resonators. The analysis reveals the influence of feed impedance and rotational orientation of a pair of coupled SRRs on the excited resonant modes, which, in turn, determine the power transfer levels between both SRRs and the frequencies at which these occur. The insights provided suggest the aptness of rotational orientation and feed impedance as critical design parameters for the realization of SRR-based magneto-inductive waveguides and wireless power transfer setups.

K e y w o r d s: characteristic-mode analysis, coupling, split-ring resonator, power transfer, transmission coefficient

1 Introductioon

Split-ring resonators (SRRs) are some of the more common fundamental metamaterial particles [1], with several configurations currently available [2]. In addition to exhibiting negative magnetic permeability features, SRRs are strongly resonant and characterized by dimensions that are significantly fractional of the free-space wavelength.

Although initially conceptualized as planar structures, significant improvements in coupling have been observed with the use of 3D SRR structures, with the potential for the realization of performance enhancements without compromising restricted footprints [3]. Characterizations of the coupling between SRR units in close proximity [4-8] have provided impetus for their application as components for magneto-inductive wave systems [9], and topologically protected resonator chains for robust wireless power transfer [10-13].

SRRs are typically multi-resonant structures, exhibiting a fundamental resonant mode in addition to other higher-order modes [14]. This characteristic is suggestive of a diversity of frequencies for resonant power transfer between a given set of coupled SRR units. Investigations of the coupling behaviour of SRR units are, however, often based on quasistatic models, thereby only accounting for the geometrically determined fundamental resonant frequency. The theory of characteristic modes, which enables an excitation-independent analysis of current modes over the surface of conducting bodies [15], has shown its utility for investigating the modal characteristics of wireless power transfer schemes [16], [17]. The intent of this paper, therefore, is to leverage on characteristic mode analysis to gain insight into the modal characteristics of coupling between SRR units, noting the frequencies at which power transfer between coupled units can be effected. This analysis involves examining the impact of the relative orientation of coupled SRR units on characteristic modes contributing to power transfer between them. It also examines the influence of feed impedance on the modal contributions. The study is executed through electromagnetic simulations in CST Microwave Studio, based on the model of a 3D SRR, which is shown in Fig. 1.

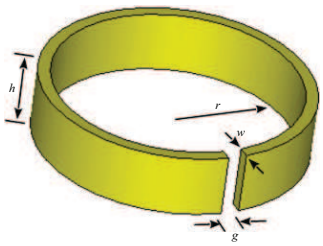

Fig. 1. 3D Circular split-ring resonator

2 Modal analysis of 3D circular split-ring resonator

Characteristic mode analysis relates surface currents J and impedances in an eigenvalue problem [18]

$$X(J_n) = \lambda_n R(J_n), \tag{1}$$

where λ_n are the eigenvalues. R and X are the real and imaginary components of the impedance matrix. For each current eigenmode J_n, the corresponding eigenvalue is

$$\lambda_n = \frac{X}{R}, \quad -\infty < \lambda_n < \infty. \tag{2}$$

For convenience, these eigenmodes are normalized as a modal significance parameter, defined as

$$m_n = \left|\frac{1}{1 + j\lambda_n}\right|, \quad 0 < m_n < 1. \tag{3}$$

[1] Department of Electrical/Electronic Engineering, University of Port Harcourt, Nigeria, akaa.eteng@uniport.edu.ng

https://doi.org/10.2478/jee-2022-0056, Print (till 2015) ISSN 1335-3632, On-line ISSN 1339-309X

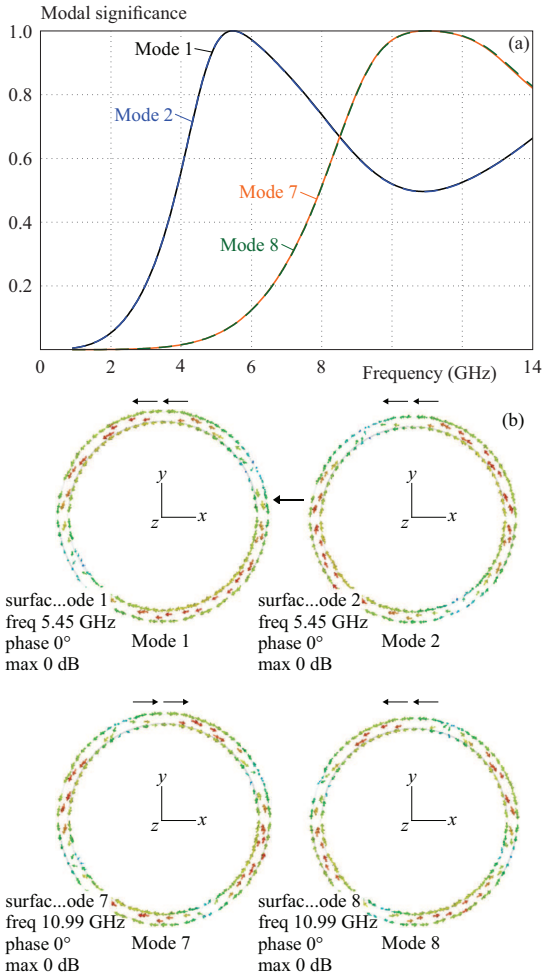

Fig. 2. Computed resonant modes in ring resonator: (a) – modal significance, (b) – surface currents of resonant modes

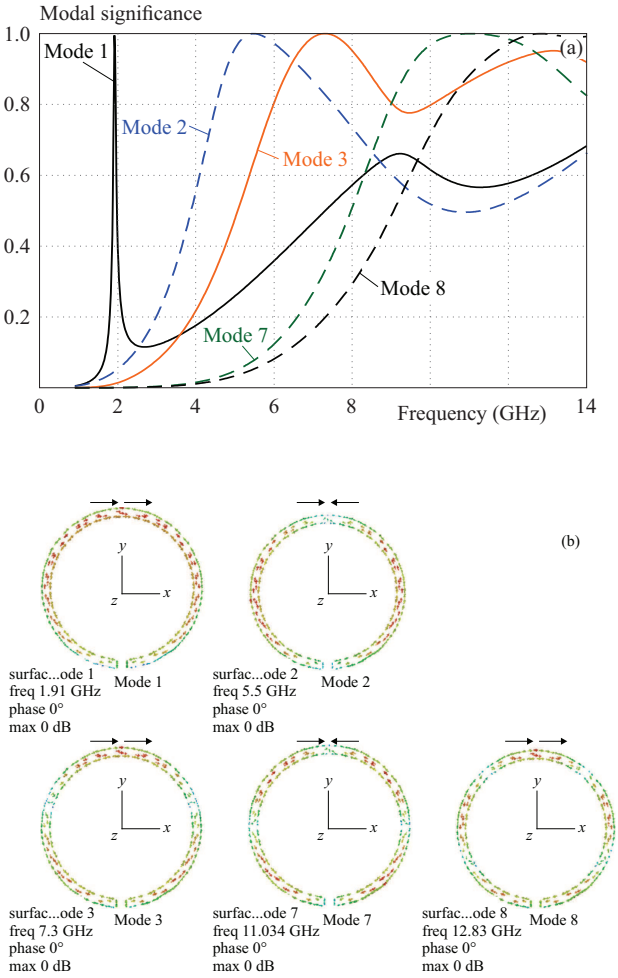

Fig. 3. Computed resonant modes in split-ring resonator (a) – modal significance; (b) – surface currents of resonant modes

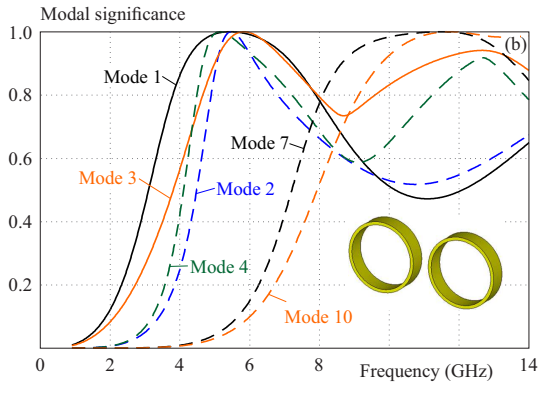

Fig. 4. Edge-coupled ring resonator modes, inlay - resonators

A characteristic mode n is resonant at the frequency where $m = 1$ $(ie, \lambda_n = 0.)$

Electromagnetic simulations in CST Microwave Studio are employed to compute the characteristic modes of the SRR structure shown in Fig. 1 ($r = 10\,\text{mm}$, $h = 5\,\text{mm}$, $w = 1\,\text{mm}$, $g = 1.5$ mm). For comparison, the same analysis is performed on a ring resonator of the same dimensions, but without a split-gap. The study then is extended to examine the characteristic modes when the SRR is coupled to its duplicate separated by a distance of 5 mm. This enables an examination of modal characteristics, and the reflection and transmission coefficients of the resulting dimer in edge- and broadside-coupled configurations at different rotational orientations. Computed modes are obtained without excitation sources and are numbered relative to their modal significance at the lowest modal resonance frequency. On the other hand, reflection and transmission coefficients are obtained from scattering parameters (s_{11}/s_{22} and s_{21}, respectively) derived by exciting SRR units through direct feeding ports connected across their split-gaps.

3 Results and discussion

3.1 CMA of ring resonator

Results of a CMA of a baseline ring resonator are presented in Fig. 2.

From Fig. 2, 4 modes in the ring resonator can be observed to have a modal significance of 1 within the observation window of 1 GHz to 14 GHz. The modes are sorted

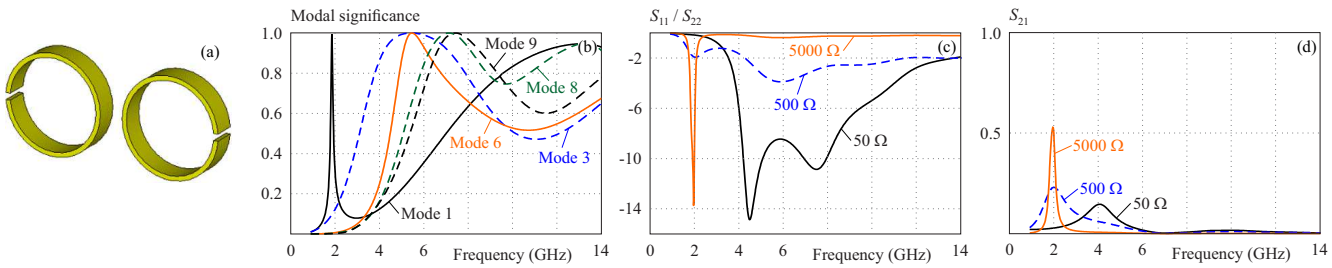

Fig. 5. Far-gap edge-coupled orientation: (a) – coupled SRRs; (b) resonant modes, (c) – reflection coefficients, (d) – transmission coefficients

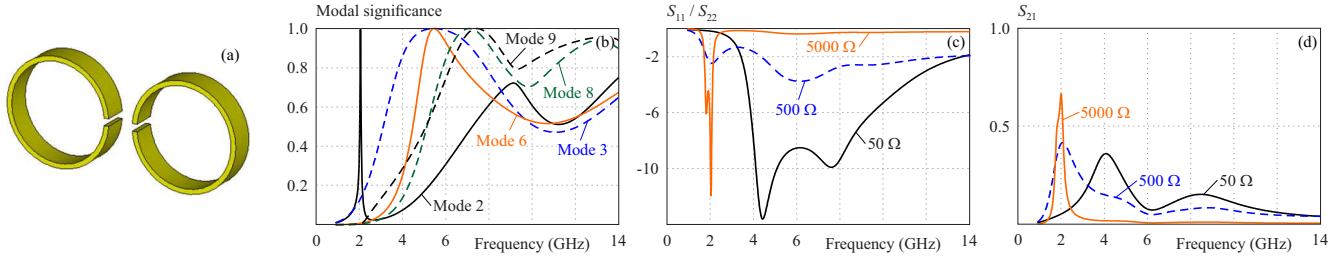

Fig. 6. Near-gap orientation: (a) – coupled SRRs, (b) – resonant modes, (c) – reflection coefficients, (d) – transmission coefficients

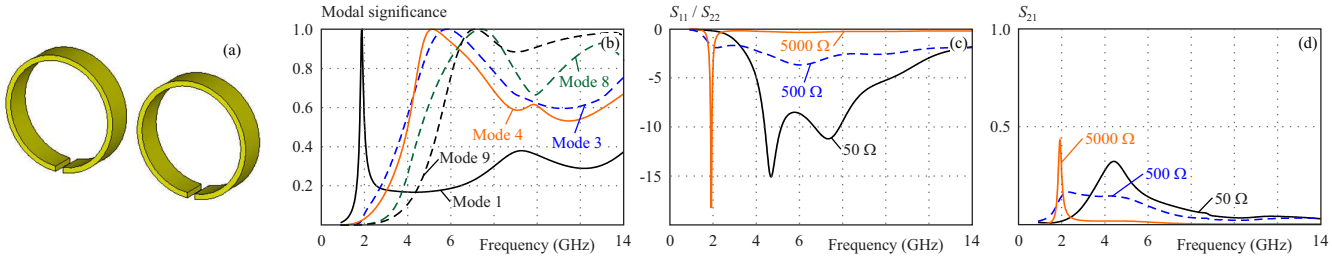

Fig. 7. Same-gap orientation: (a) – coupled SRRs, (b) – resonant modes, (c) – reflection coefficients, (d) – transmission coefficients

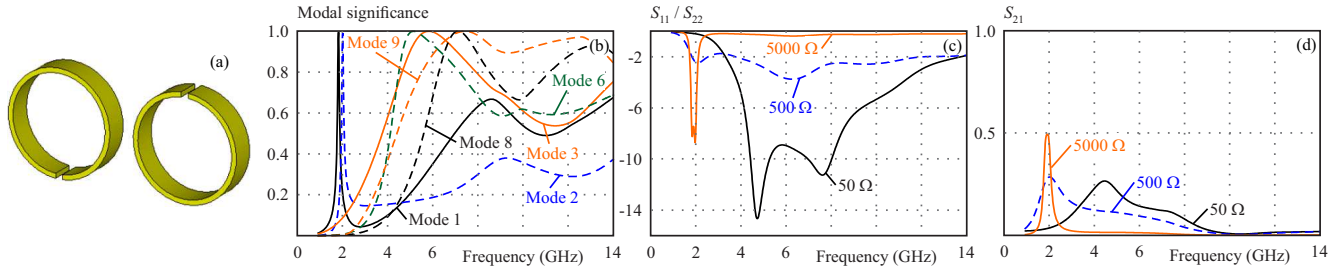

Fig. 8. Opposite-gap orientation: (a) – coupled SRRs, (b) – resonant modes, (c) – reflection coefficients, (d) – transmission coefficients

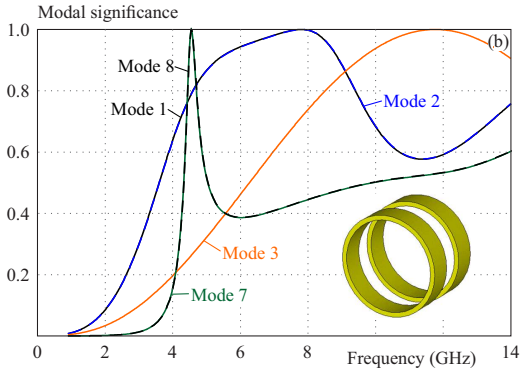

Fig. 9. Broadside-coupled ring resonator modes, inlay – resonator

according to their significance at 5.45 GHz, which in this case, is the lowest resonance frequency. Modes 1 and 2 are coincident, and resonate at 5.45GHz. Both modes are also even, with symmetric surface currents provided at the $\phi = 0$ position on the ring resonator. Modes 7and 8 are likewise coincident, resonate at 10.99GHz, and are symmetric at the $\phi = 0$ position, with current directions as indicated by the black arrows. Two nulls each are associated with modes 1 and 2, while modes 7 and 8 are each characterized by 4 nulls.

3.2 CMA of split-ring resonator

In contrast to the modal characteristics of the ring resonator, the split ring resonator has an additional significant narrowband mode, excited at a lower frequency of 1.91 GHz. Other significant modes are excited at frequencies close to the modal resonances observed with the

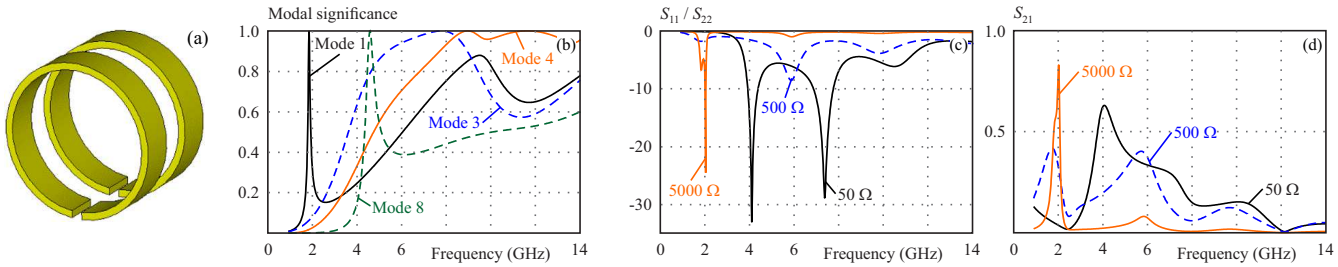

Fig. 10. Same-gap orientation: (a) – coupled SRRs, (b) – resonant modes, (c) – reflection coefficients, (d) – transmission coefficients

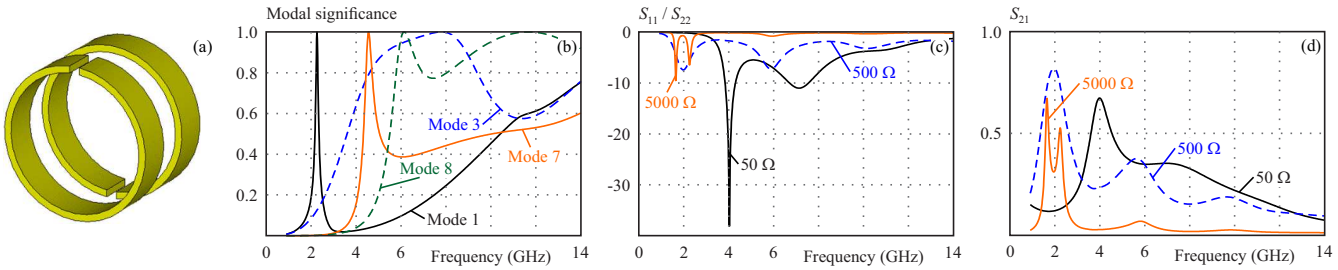

Fig. 11. Opposite-gap orientation: (a) – coupled SRRs, (b) – resonant modes, (c) – reflection coefficients, (d) – transmission coefficients

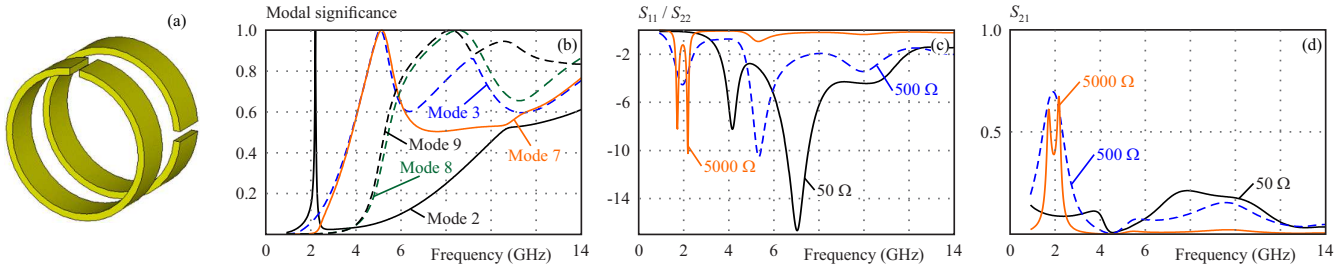

Fig. 12. Perpendicular-gap orientation: (a) – coupled SRRs, (b) – resonant modes, (c) – reflection coefficients, (d) – transmission coefficients

ring resonator, but with no two modes coincident. As shown in Fig. 3, the resonant modes for the SRR are modes 1, 2, 3, 7, and 8, resonating at 1.91 GHz, 5.5 GHz, 7.3 GHz, 11.0 GHz, and 12.8 GHz. Fundamentally, the excitation of mode 1, and the non-coincidence of the other resonant modes can be attributed to the presence of the gap in the SRR structure. The current flow associated with mode 1 is even, and unidirectional throughout the SRR. However, other modes are characterized by nulls within the structure, with corresponding reversals in the direction of current flow. Modes 2 and 7 are odd, with asymmetrical current flows at the $\phi = 0$ position. These modes are characterized by 2 and 4 nulls, respectively. Modes 3 and 8 are even, with 2 and 4 nulls, respectively. It is noteworthy that the odd modes have nulls positioned around the gap.

3.3 CMA of edge-coupled ring resonators

Edge-coupling of a pair of the modelled ring resonators results in six resonant modes appearing between 1 GHz and 14 GHz, as shown in Fig. 4. However, the resonances of these modes are clustered around two bands. The lower order modes, modes $1-4$, resonate between $4-6$ GHz, while modes 7 and 10 resonate between $10.4-14$ GHz.

3.4 CMA of edge-coupled SRRs

Figures 5 to 8 reveal the resonant characteristic modes excited in a pair of edge-coupled SRRs placed 5mm apart. The results reveal the consistent presence of a narrowband resonant characteristic mode at 1.9GHz, irrespective of the rotational orientation of the edge-coupled SRR units. Other significant modes are likewise resonant within the 4 to 8 GHz window. Similarly, the reflection coefficient results reveal that both coupled SRR units have reflection coefficient minima at 1.9 GHz, and between 4 GHz and 8 GHz. The corresponding transmission coefficient plots reveal that the feed impedance plays a crucial role in determining what modes contribute to a high transmission coefficient between the coupled SRRs. As a consequence of the clusters of mode resonances, transmission coefficient peaks are either at 1.9 GHz or 4.5 GHz, depending on the feed impedance. Higher feed impedances are required to excite mode 1, and mode 2 in Fig. 8, resulting in the narrowband higher level transmission coefficient at 1.9 GHz. Conversely, the

transmission coefficient peak at 4.5 GHz, is characterized by a lower transmission coefficient, and broader bandwidth, due to contributions of multiple overlapping modes excited through a much lower feed impedance level. Of the four edge-coupled orientations examined, the highest transmission coefficient of 0.67 is realized using the near-gap orientation, and a high feed impedance of 5 kΩ. It is important to observe that lower values of reflection coefficients at the SRR units do not necessarily translate to higher transmission coefficients between them, see Fig. 7 and Fig. 8.

3.5 CMA of broadside-coupled ring resonator

For the broadside-coupled ring resonators, five resonant modes are excited between 1 GHz and 14 GHz. These consist of two pairs of coincident modes - modes 1 and 2 resonating at 7.7 GHz, and modes 7 and 8 resonating at 4.6 GHz. These are complemented by a single mode resonating at 11.7 GHz.

3.6 CMA of broadside-coupled SRR

Similar to the case of edge-coupled SRRs, there is a consistent characteristic mode resonating at 1.9 GHz. This mode is excited for power transfer through the use of a high feed impedance (5 kΩ in this case). The highest transmission coefficient is realized at 1.9 GHz, and an overall best value of 0.83 is achieved with the same-gap orientation and 5 kΩ feed impedance, Fig. 10. However, in contrast to the edge-coupled configuration, rotational orientation exerts influence on the feed impedance required to maximize transmission at this frequency. In Figures 11 and 12, the highest transmission coefficient is realized using 500 Ω Using 5 kΩ as the feed impedance leads to frequency splitting, and a lower transmission coefficient. Comparing the overlap between modes 1 and 8 within 2 GHz − 4 GHz in Fig. 10, to that occurring between modes 1 and 7 within the same frequency range in Figures 11 and 12, one can deduce that frequency splitting occurs when two characteristic modes resonate at close frequencies, but without significant overlap. Overall, broadside coupling of SRRs generally results in lower reflection coefficients and higher transmission coefficients compared to edge coupling orientations.

4 Conclusions

This paper has employed the CMA technique to examine frequency characteristics of coupling between a pair of SRRs. To this end, characteristic modes of edge-coupled and broadside-coupled SRR units have been computed for various rotational orientations, and compared with the modal characteristics of baseline ring resonator configurations. Furthermore, reflection and transmission coefficients of these SRR coupling orientations have been derived on the basis of feed excitations at the split-gaps. The results reveal that broadside coupling of SRR units, in general, provides higher transmission coefficients than edge coupling setups. Furthermore, it is observed that the split-gap in an SRR structure introduces a lower frequency characteristic mode, which is absent in ring resonators. This mode, which can be excited using a high feed impedance, presents an avenue for narrow-band higher-level power transfer at its resonant frequency. Lastly, frequency splitting in the transmission coefficient, which is indicative of high-level coupling, is synonymous with two characteristic modes resonating at close frequencies, but without significant overlap between themselves. Consequently, the suppression of either of these two modes will lead to the elimination of the transmission coefficient frequency-split. In conclusion, the application of CMA to coupled SRRs in this study has shown what resonances are possible, and the frequencies at which power transfer can be effected. This study reveals that at a given separation distance, power transfer between a pair of SRR units can be controlled using two parameters - rotational orientation and feed impedance. These two parameters can therefore be applied as prime tools for the design of SRR-based magento-inductive waveguides, and wireless power transfer links.

References

[1] D. R. Smith, J. B. Pendry, and M. C. K. Wiltshire, "Metamaterials and negative refractive index", *Science*, vol. 305, no. 5685, pp. 788-792, 2004.

[2] R. Marques, F. Martin, and M. Sorolla , *Metamaterials with Negative Parameters Theory, Design and Microwave Application*, Hoboken, New Jersey: John Wiley & Sons, Inc., 2008.

[3] A. Vallecchi, C. J. Stevens, and E. Shamonina, "3D coupled resonators for enhanced filter design", *IET Conf. Publications*, no. CP741, pp. 6-9, 2018.

[4] F. Hesmer *et al*, "Coupling mechanisms for split ring resonators: Theory and experiment", *Physica status solidi* B, vol. 244, no. 4, pp. 1170-1175, 2007.

[5] N. Feth *et al*, "Electromagnetic interaction of split-ring resonators: The role of separation and relative orientation", *Optics Express*, vol. 18, no. 7, pp. 6545, 2010.

[6] S. S. Seetharaman, C. G. King, I. R. Hooper, and W. L. Barnes, "Electromagnetic interactions in a pair of coupled split-ring resonators", *Physical Review* B, vol. 96, no. 8, pp. 1-7, 2017.

[7] F. Zhang, Q. Zhao, J. Sun, J. Zhou, and D. Lippens, "Coupling effect of split ring resonator and its mirror image", *Progress in Electromagnetics Research*, vol. 124, January, pp. 233-247, 2012.

[8] M. Baraclough, I. R. Hooper, and W. L. Barnes, "Investigation of the coupling between tunable split-ring resonators", *Physical Review B*, vol. 98, no. 8, pp. 085146, 2018.

[9] S. Chu, M. S. Luloff, J. Yan, P. Petrov, C. J. Stevens, and E. Shamonina, "Magnetoinductive waves in attenuating media", *Scientific Reports*, pp.11-12, 2021.

[10] Z. Guo, H. Jiang, Y. Sun, Y. Li, and H. Chen, "Asymmetric topological edge states in a quasiperiodic Harper chain composed of split-ring resonators", *Optics Letters*, vol. 43, no. 20, pp. 5142, 2018.

[11] Z. Guo *et al*, "Rotation controlled topological edge states in a trimer chain composed of meta-atoms", *Journal of Physics* , vol. 24, no. 6, pp. 063001, 2022.

[12] J. Feis, C. J. Stevens, and E. Shamonina, "Wireless power transfer through asymmetric topological edge states in diatomic chains of coupled meta-atoms", *Applied Physics Letters*, vol. 117, no. 13, pp. 134106, 2020.

[13] J. Jiang *et al*, "Experimental demonstration of the robust edge states in a split-ring-resonator chain", *Optics Express* , vol. 26, no. 10, pp. 12891, 2018.

[14] J. Garca-Garca, F. Martn, J. D. Baena, R. Marqus, and L. Jelinek, "On the resonances and polarizabilities of split ring resonators", *Journal of Applied Physics*, vol. 98, no. 3, p. 033103, 2005.

[15] M. Cabedo-Fabres, E. Antonino-Daviu, A. Valero-Nogueira, and M. F. Bataller, "The theory of characteristic modes revisited: A contribution to the design of antennas for modern applications", *IEEE Antennas and Propagation Magazine*, vol. 49, no. 5, pp. 52-68, 2007.

[16] F. Abderrazak, E. Antonino-Daviu, M. Ferrando-Bataller, L. Talbi, and A. Al Qaraghuli, "A Comparative Study between Different Loop Antennas Topologies for Wireless Power Transmission based on Modal Analysis", *15th European Conference on Antennas and Propagation (EuCAP*, pp. 1-5, 2021.

[17] F. Abderrazak, E. Antonino-Daviu, and M. Ferrando-Bataller, "Power Transfer Efficiency Analyzed using Characteristic Mode Coupling Between Two Parallel Loops", *2020 14th European Conference on Antennas and Propagation (EuCAP*, pp. 1-5, 2020.

[18] M. Vogel, G. Gampala, D. Ludick, and C. J. Reddy, "Characteristic Mode Analysis: Putting Physics back into Simulation", *IEEE Antennas and Propagation Magazine*, vol. 57, no. 2, pp. 307-317, 2015.

Received 10 August 2022

Akaa Agbaeze Eteng obtained a BEng degree in Electrical/Electronic Engineering from the Federal University of Technology Owerri, Nigeria in 2002, and a MEng degree in Telecommunications and Electronics from the University of Port Harcourt, Nigeria in 2008. In 2016, he obtained a PhD in Electrical Engineering from Universiti Teknologi Malaysia. He is currently a lecturer at the Department of Electrical/Electronic Engineering at the University of Port Harcourt, Nigeria. His research interests include wireless energy transfer, radio frequency energy harvesting, and wireless powered communications.